LA-UR-85-1627

AUG 07 1985
CONF-8505164--3

Los Alamos National Laboratory is operated by the University of California for the United States Department of Energy under contract W-7405-ENG-36

TITLE: SCHEME TO FUNNEL ION BEAMS WITH A RADIO-FREQUENCY QUADRUPOLE

LA-UR--85-1627

DE85 015689

AUTHOR(S): R. H. Stokes and G. N. Minerbo

SUBMITTED TO: Workshop on High Brightness, High Current, High Duty Factor Ion Injectors in San Diego, California, May 21-23, 1985.

SCHEME TO FUNNEL ION BEAMS
WITH A RADIO-FREQUENCY QUADRUPOLE*

R. H. Stokes and G. N. Minerbo,† MS H817
Los Alamos National Laboratory, Los Alamos, NM 87545

ABSTRACT

We describe a proposed method to funnel ion beams using a new form of the radio-frequency quadrupole (RFQ) structure. This RFQ accepts two bunched ion beams and combines them into a single final beam with interlaced microstructure pulses. It also provides uninterrupted periodic transverse focusing to facilitate the funneling of beams with high current and low emittance.

INTRODUCTION

Several new linear-accelerator applications require output ion beams with very high current and small transverse emittance. The transverse beam brightness (beam current divided by the product of the x- and y-emittances) is often used as the figure of merit, and the design objective is to obtain a very high brightness output beam. When linear-accelerator channels operate near their space-charge limit, one method to increase brightness is to combine the beams from two (or more) space-charge-limited channels. The resultant beam would have interlaced microstructure bunches and would be suitable for further acceleration in a linac operating with twice the frequency. This operation has been called funneling and was first proposed as a necessary part of the rf linac approach to heavy-ion fusion.[1] If the funneling of two beams is accomplished with no transverse emittance growth or beam loss, the resulting beam will have twice the current and twice the brightness of the beams that are combined. Increasing beam brightness through funneling requires no improvement in the ion source or accelerator techniques used before the funneling process.

In some applications, to meet brightness requirements, one could use arrays having multiple beams traversing the whole accelerator system with the final beams all focused to a common target spot. If the required brightness were not too high, funneling to combine multiple beams as early as possible would be especially advantageous in large accelerators where most of the acceleration could then be provided in a minimum-cost single-beam accelerator. In general this single-beam accelerator would be less complex and would require less rf power than designs that carry all the initial beams through the entire accelerator system. A funneling tree to combine four beams is shown in Fig. 1. In practice, funneling to increase beam brightness is a difficult

*Work supported by the US Department of Energy.
†Now with Schlumberger, Houston Engineering Center.

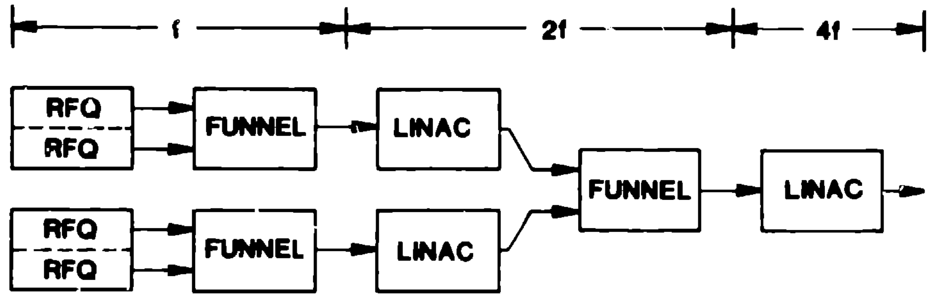

Fig. 1. Funneling tree.

design problem. Initial work using discrete optical elements has been done by Bongardt[2] and by Guy and Wangler.[3]

In 1981, we suggested[4] that ion beams could be funneled with an RFQ of special design. This paper discusses use of this RFQ for the funnel stages (shown in Fig. 1) immediately following the RFQ accelerators. In a funneling tree, the first type of funnel following the RFQ accelerator is present in greater numbers than all other types combined, so it is especially important that a capable and efficient design be developed. Instead of discrete optical elements, we propose to funnel entirely within the special RFQ structure so that the beams are always contained by uninterrupted periodic focusing. Beams with high space charge experience irreversible emittance growth when they emerge from a periodic focusing system or when their focusing periodicity is abruptly changed. To alleviate this problem, in the proposed funneling scheme it should be possible to provide uninterrupted focusing with the same periodicity as that of the accelerators preceding the funnel. Also, instead of conventional deflection systems, we propose to use the properties of the special RFQ structure to deflect two parallel beams toward each other and to merge them into a single final beam. This funneled beam would then be suitable for further acceleration in a linac with twice the frequency of the RFQ funnel. The initial RFQ accelerator, the RFQ funnel, and the following linac would all have every longitudinal bucket filled with ion bunches, and the capability of the accelerator system would be fully utilized.

BEAM DEFLECTION IN PERIODIC FOCUSING CHANNELS

Our first objective was to devise a method to produce transverse deflections of a beam traveling in a periodic focusing system such as an RFQ. We found that introducing periodic transverse displacements of the focusing and defocusing lenses was very effective in producing a deflecting force. To develop this idea, we used the thin-lens array shown in Fig. 2. The input beam

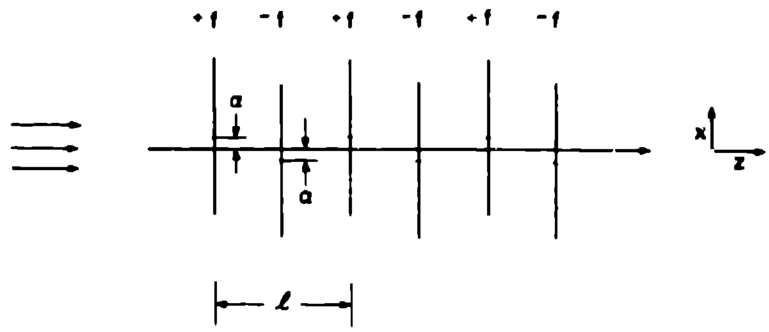

Fig. 2. Periodic thin-lens array used for simulation.

first traversed a focus lens whose center was displaced in the plus x-direction by an amount a. Next was a defocus lens displaced in the minus x-direction by the same amount, etc. The lenses had focal length f and were equally spaced with focusing period ℓ. This arrangement produces a net force on the beam in the plus x-direction. To determine the beam optical properties, we performed single-particle simulations. We learned that such alternating lens displacements produce a displaced neutral axis about which sinusoidal betatron motion takes place. The betatron frequency is independent of a; thus, in the spirit of the smooth approximation, there exists a constant average transverse force, and the betatron motion corresponds to that of a biased, simple harmonic oscillator.

In Fig. 3, the curve labeled $a = 0$ shows the usual betatron motion about the z-axis. The particle started at the origin with a

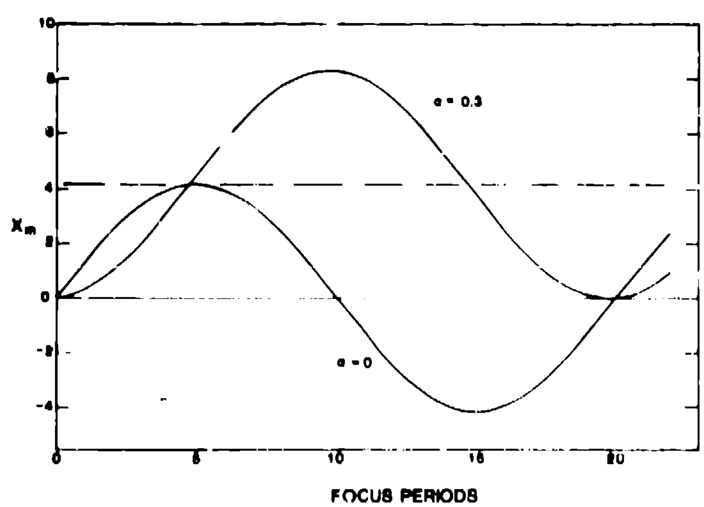

Fig. 3. Particle trajectories showing the effect of transverse lens displacements. With $a = 0$, the betatron motion is centered on the z-axis. With $a = 0.3$, the motion is centered about a displaced neutral axis.

positive initial slope and the parameters were $\alpha = 0$, $f = 16$, and $\ell = 10$. The betatron period is 20 focus periods and the curve is plotted through the points of maximum flutter motion. Also in Fig. 3, for $f = 16$ and $\ell = 10$, we show a curve for transversely displaced lenses with $\alpha = 0.3$. The particle started at the origin with zero slope, and again the curve was plotted through the points of maximum flutter. The curve is sinusoidal about a displaced axis and has the same betatron frequency as for $\alpha = 0$. In Fig. 4, we have plotted this same $\alpha = 0.3$ curve in more detail, along with an explanation of the motion. The top and bottom curves are drawn respectively through the maxima and the minima of the flutter motion. The average of these two curves is symmetric about the dashed neutral axis that is displaced from the z-axis by x_d. Note that the trajectory flutter is zero on the z-axis, increases to $\pm\alpha$ at $x = x_d$, and to $\pm 2\alpha$ at $x = 2x_d$. The left part of the figure explains these effects. In the smooth approximation, the transverse forces are proportional to the amplitude of the flutter motion. The trajectory flutter produces a restoring force proportional to the displacement from the z-axis. The lens flutter produces a constant (dipole) force of magnitude proportional to α, and these forces balance at $x = x_d$, producing the displaced neutral axis. The algebraic sum of forces from the two types of flutter then produces a restoring force that is linear relative to displacements from the neutral axis. Further,

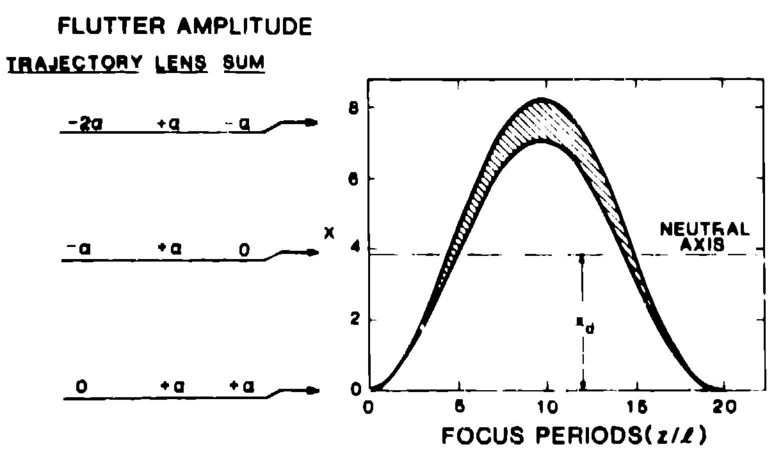

Fig. 4. Results of a thin-lens simulation with transverse alternating lens displacements of amplitude α. Initially, the particle was injected with zero slope at the origin. The upper and lower curves are plotted through the maxima and the minima of the trajectory flutter. The betatron motion is sinusoidal about the displaced neutral axis with a period independent of α. Amplitudes of the trajectory flutter, lens flutter, and their sum are shown on the left.

the betatron frequency is independent of α, so that the focusing properties are preserved.

To confirm that a displaced neutral axis exists, we simulated a particle starting at $x = x_d + \alpha$. For a proper choice of initial slope, the particle traveled along the lens system with flutter half-amplitude equal to α and with zero betatron amplitude, showing that forces from the lens and trajectory flutters exactly balance. It can be shown that the neutral axis displacement for this thin-lens system is $x_d = 8\alpha f/\ell$.

Next, we formulated a smooth-approximation calculation to describe these effects. The calculations correspond to an rf quadrupole focusing system that has successive lenses displaced transversely from the z-axis. We used a sine-wave displacement function of amplitude α and space period $\beta\lambda = 2\pi v/\omega$, where v is the particle velocity and ω is the rf quadrupole operating frequency. The appropriate differential equation is

$$M \frac{d^2x}{dt^2} + K(x - \alpha \sin \omega t) \sin \omega t = 0 \quad , \tag{1}$$

where K is the spring constant and M the particle mass. If $\alpha = 0$, Eq. (1) reduces to one form of the Mathieu equation used to describe periodic focusing. We assume a solution of the form

$$x = R \sin \Omega t + S \sin \omega t + x_d \quad , \tag{2}$$

where the first term represents the betatron motion, the second term the flutter, and x_d is the displacement of the neutral axis. If we take R>>S, and $\omega \gg \Omega$ (the smooth approximation), we obtain

$$S = \left(\frac{\omega_0}{\omega}\right)^2 (R \sin \Omega t + x_d) \quad , \quad \text{where} \quad \omega_0^2 = K/M \quad .$$

After substituting this into Eq. (2), Eq. (2) into Eq. (1), and then averaging the terms over one rf period, we find the equation satisfied if both

$$\Omega = \frac{\sqrt{2}}{2} \frac{\omega_0^2}{\omega} \quad , \quad \text{and} \quad x_d = \alpha\left(\frac{\omega}{\omega_0}\right)^2 = \frac{\sqrt{2}}{2} \alpha\left(\frac{\omega}{\Omega}\right) \quad . \tag{3}$$

First we see that the betatron frequency Ω is independent of α. Next we observe that x_d is equal to α multiplied by the factors $(\sqrt{2}/2)(\omega/\Omega)$. Because $\omega \gg \Omega$, then $x_d \gg \alpha$, which demonstrates that small transverse displacements are very effective in producing large displacements of the neutral axis. Although we have used the smooth approximation to obtain simple expressions for Ω and x_d, neither the beam manipulations discussed below nor the funneling scheme discussed later are necessarily limited to the region where the smooth approximation is valid.

Now we discuss the use of this deflection force to sidestep a beam from the z-axis to a displaced parallel axis. In doing this, we must use a method that does not induce additional betatron motion that would increase the beam emittance. One possible method is to start with a particle moving along the z-axis and, at the origin, turn on an initially constant value of α to induce a half-period betatron motion. When this excursion reaches its full amplitude, we then suddenly double the value of α to move the neutral axis to a point equal to the betatron amplitude. This procedure results in the displaced trajectory shown in Fig. 5, curve (a), where the curve is the mean of the flutter motion. After α has reached its final value of 0.6, this trajectory has a residual betatron amplitude of only 0.05% for the particular manner in which α was programmed. Alternatively, the particle could be injected along the displaced neutral axis with $x = 7.7$ and $\alpha = 0.6$. Then by reducing α in a programmed manner, the particle could be brought to the z-axis with zero slope. This sidestep maneuver forms one-half of the funneling scheme that in the next section will be extended so that two beams can be brought to a common z-axis. Also shown in Fig. 5 are curves (b) and (c) for which the motion was started with initial ± slopes. The amplitude of the resulting betatron motion about the displaced axis is equal to the case with $\alpha = 0$, showing that the sidestep maneuver produces no increase in the transverse emittance.

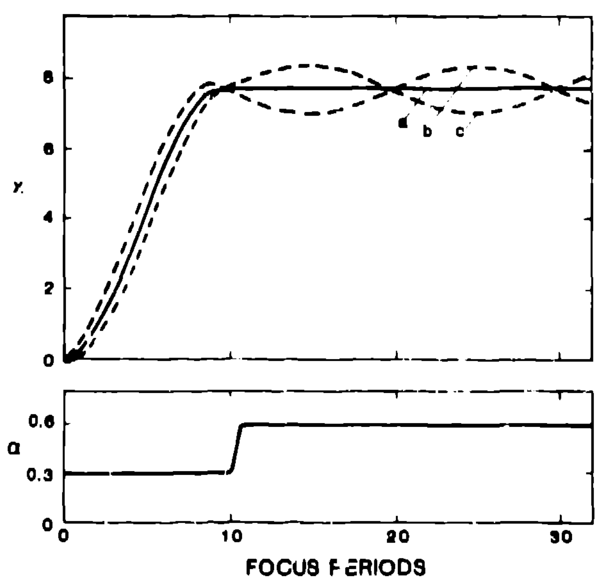

Fig. 5. Sidestep maneuver to displace a beam without increasing the transverse emittance. Particle (a) is injected with zero slope at the origin. Initially, a constant transverse force is applied through an alternating lens displacement of amplitude $\alpha = 0.3$. After one-half period of the betatron motion, the value of α is doubled to make the neutral axis coincide with the betatron maximum amplitude. The result is a trajectory displaced 7.7 units from the z-axis with negligible residual betatron amplitude. Particles (b) and (c) are injected with finite slope. They have the same amplitude as when $\alpha = 0$.

RFQ POTENTIAL FUNCTIONS

The conventional RFQ accelerator was proposed and developed in a somewhat unusual manner.[5,6] Instead of initially specifying the electrode geometry, a potential function was synthesized to give electric fields with the required beam-dynamical properties. Then, both the electric-field distributions and the isopotential shapes corresponding to the RFQ poles were derived from the potential function. We follow the same procedures in developing a new type of RFQ structure that has the beam-dynamical properties needed to funnel ion beams.

The standard RFQ accelerator potential function can be written in cylindrical coordinates (r, ψ, z) as

$$U = \frac{V}{2} \left[X \left(\frac{r}{a}\right)^2 \cos 2\psi + A I_0(kr) \cos kz\right] \sin(\omega t + \phi) \quad , \qquad (4)$$

where V is the maximum potential difference between adjacent pole tips and $k = 2\pi/\beta\lambda$. Note that the I_0 Bessel function is even and symmetric in x and y. To provide a deflection force in the x-direction, we require I_0 to be replaced with a function that is odd in x and independent of y. Also, the potential function chosen must satisfy Laplace's equation. One example meeting these requirements is

$$U = \frac{V}{2} \left[C \left(\frac{x^2 - y^2}{a^2}\right) + D \sinh kx \cos kz\right] \sin(\omega t + \phi) \quad , \qquad (5)$$

where the quadrupole focusing term is the same as in Eq. (4) but written in x-y coordinates. Another potential function is discussed in Appendix A.

The electric field components calculated from Eq. (5) are

$$E_x = -\frac{CV}{a^2} x - \frac{kDV}{2} \cosh kx \cos kz \ , \quad E_y = \frac{CV}{a^2} y \ , \quad E_z = \frac{kDV}{2} \sinh kx \sin kz \ ,$$

with each component multiplied by $\sin(\omega t + \phi)$. The second term in the expression for E_x produces a deflection force. The field averages taken over a $\beta\lambda$ period, for a synchronous particle with x and y held constant, are

$$\bar{E}_x = -\frac{kDV}{4} \cosh kx \sin \phi \ , \quad \bar{E}_y = 0 \ , \quad \bar{E}_z = \frac{kDV}{4} \sinh kx \cos \phi \ .$$

Figure 6 compares the x-z plane pole-tip shape of the funneling RFQ with that of the conventional RFQ accelerator. The pole-tip shape of a funneling RFQ is discussed in Appendix B. The results of a numerical computation in the x-z plane are shown in Fig. 7. For the same parameters as Fig. 7, Fig. 8 shows the pole-tip shape in the x-y plane for three values of z. The transverse displacement of the pole tips in the x-direction with period $\beta\lambda$ is the analogue of the thin-lens displacements of Fig. 2.

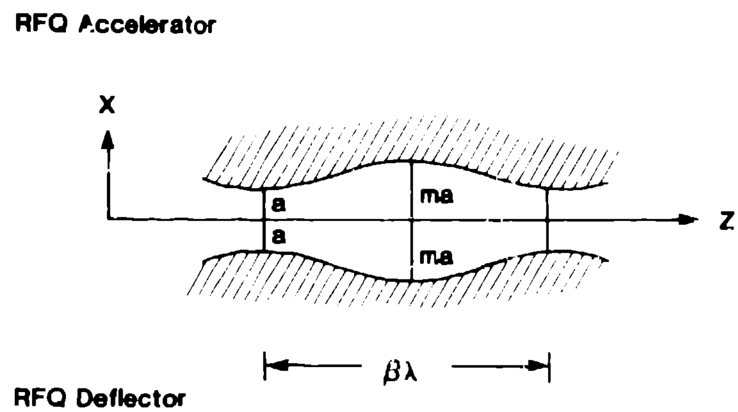

Fig. 6. Comparison of pole shapes in the x-z plane for an RFQ accelerator and for an RFQ deflector that can be used to funnel ion beams.

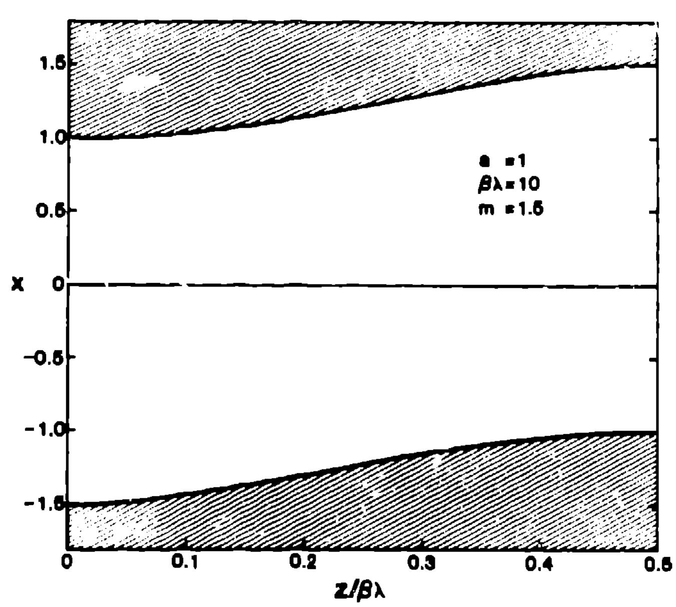

Fig. 7. Computed RFQ funnel pole-tip shape in the x-z plane.

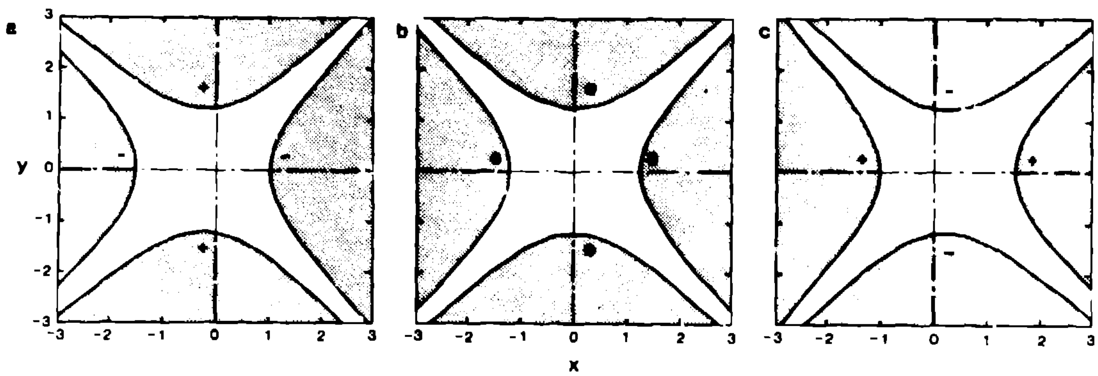

Fig. 8. An RFQ funnel pole-tip shape in the x-y plane at the beginning (a), middle (b), and end (c) of a unit cell of length $\beta\lambda/2$. The curves are from a numerical solution of Eq. (A-1) for a = 1, m = 1.5, and $\beta\lambda$ = 10. The polarities shown correspond to a bunched beam with $\phi = -90°$. In addition to the usual quadrupole focusing forces, the beam will experience a deflecting force in the positive x-direction.

If we use the force corresponding to the above expression for E_x, the Mathieu equation becomes

$$\frac{d^2x}{dt^2} + \frac{qCV}{Ma^2}\left[x + \frac{ka^2D}{2C}\cosh kx \cos kz\right]\sin(\omega t + \phi) = 0 \quad . \qquad (6)$$

From a smooth-approximation calculation for a particle with synchronous velocity ($kz = \omega t$) and for $kx \ll 1$, so that $\cosh kx \simeq 1$, we obtain expressions for the betatron frequency Ω and for the displacement of the neutral axis x_d:

$$\Omega = \frac{\sqrt{2}}{2}\frac{\omega_c^2}{\omega} \; , \qquad x_d = \alpha\left(\frac{\omega}{\omega_0}\right)^2 = \frac{\sqrt{2}}{2}\,\alpha\left(\frac{\omega}{\Omega}\right) \; ,$$

where now

$$\omega_0^2 = \frac{qCV}{Ma^2} \; , \qquad \text{and} \qquad \alpha = -\frac{ka^2D}{2C}\sin\phi \quad .$$

These expressions show that the position of the neutral axis is proportional to $-\sin\phi$. If we introduce a bunched ion beam with $\phi = -90°$, x_d is positive and these ions can travel along their positively displaced neutral axis parallel to the z-axis. If another ion beam contains bunches with $\phi = +90°$, x_d is negative and these ions can travel along their negatively displaced neutral axis parallel to the z-axis. Therefore, we can inject two bunched beams having their microstructure bunches displaced by $\Delta z = \beta\lambda/2$ and have them travel along separate parallel trajectories displaced $\pm x_d$ from the z-axis. Both displaced beams will be transversely focused with the same strength about their respective neutral axes. We can then funnel by reducing the deflection parameter D to zero (by decreasing m, the pole modulation parameter, to unity). This enables us to bring the two beams to the z-axis in a programmed manner that induces no additional betatron amplitude. The transverse focusing is maintained for both beams throughout this process.

Beams injected into an RFQ funnel must be closely spaced to allow the RFQ aperture to be as small as possible. The beams could originate in a conventional RFQ structure that has a single rf resonator with multiple RFQ channels. Also, the two preceding accelerator channels could be designed with a sidestep near the output to bring their beams closer to the z-axis of the funnel. If the initial beams are not closely spaced, two RFQs based on Eq. (5) can be used to "pipe" the individual beams to the RFQ funnel. Alternatively, a periodic focusing system of static electric or magnetic quadrupoles (with their centers having programmed periodic transverse displacements) could be used, together with appropriate bunchers to prepare both beams for the final funneling operation. A septum magnet placed just before the funnel may also be necessary.

The expression for E_z is similar to that of a conventional rf linac for which the expression would be $E_0T \cos \phi$, where E_0 is the space average accelerating field and T is the transit-time factor. Because sinh kx is positive for positive x-displacement, such a beam will be bunched in a manner similar to a conventional linac beam with the added feature that the bunching forces are proportional to sinh kx. For $\phi = -90°$, the beam with positive x-displacement will experience both maximum positive-displacement forces and maximum bunching. Similarly, for $\phi = +90°$, the beam with negative x-displacement will experience both maximum negative-displacement forces and maximum bunching. The operating points for these two displaced beams are shown as asterisks in the Fig. 9 diagram, which portrays the full range of possible operating conditions. As the two beams approach the funneling vertex, the bunching forces are reduced to zero. If simulation studies show this to be a serious problem, it may be possible to devise an auxiliary method to maintain adequate bunching in the vertex region. One method to avoid possible debunching effects is to funnel rapidly. In the next section, we show an example where only one-fifth of a betatron period is required. Another possibility is to excite the poles of the funneling RFQ with both the fundamental and twice the fundamental frequency. The additional frequency would allow the superposition of pole-tip modulation required to produce conventional bunching forces on the microstructure pulses, which now have $\beta\lambda$ spacing at the double frequency. The bunching force would have an I_0 Bessel function radial dependence and would be effective at all radii within the RFQ bore.

This type of structure can also serve as a two-beam accelerator. Two beams having bunches spaced $\beta\lambda/2$ can be injected along neutral axes displaced from the z-axis by $\pm x_d$. For example, if the RFQ is designed so that the beams at $+x_d$ has $\phi = -45°$, and the beam at $-x_d$ has $\phi = +135°$, the expression for

$$\bar{E}_x = -\frac{kDV}{4} \cosh kx \sin \Phi$$

$$\bar{E}_z = \frac{kDV}{4} \sinh kx \cos \Phi$$

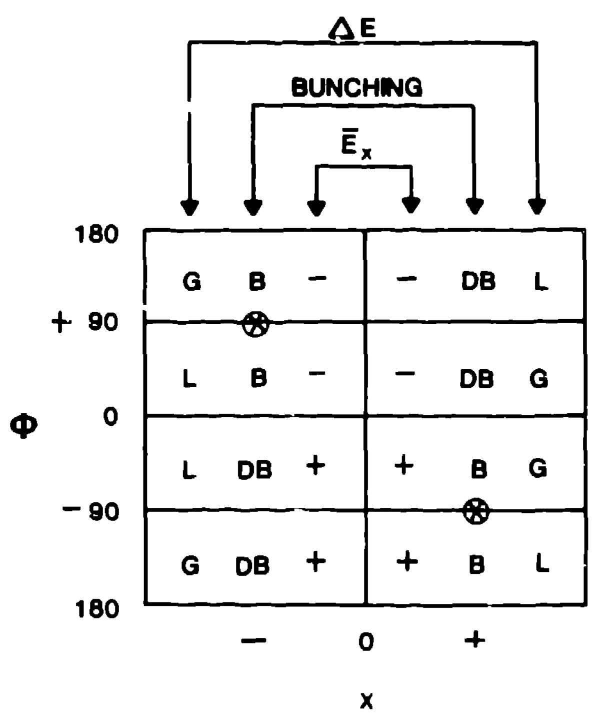

Fig. 9. Diagram showing the full range of operating conditions that are possible with a funneling RFQ. The energy gain G or loss L, the bunching B or debunching DB, and the sign of the transverse deflecting field $\bar{E}_x$ are shown as a function of the beam displacement x, and the synchronous phase ϕ.

$\bar{E}_x$ and $\bar{E}_z$ show that both beams will be accelerated, in addition to being bunched, focused, and held in displaced trajectories.

FUNNELING EXAMPLE

If we neglect space charge, funneling trajectories can be obtained by integrating both the transverse equation, Eq. (6), and the equation obtained using the longitudinal field E_z:

$$\frac{d^2z}{dt^2} - \frac{qVkD}{2M} \sinh kx \sin kz \sin (\omega t + \phi) = 0 \quad .$$

An unoptimized set of parameters was chosen to demonstrate the general properties. Protons of 2-MeV energy entered a 100-MHz RFQ funnel with an aperture parameter $a/\sqrt{C}$ = 33 mm. The peak voltage between RFQ poles was 264 kV, corresponding to a peak surface field of about 10 MV/m, and a betatron phase advance of 15° in the focus period of $\beta\lambda$ = 196 mm. The results are shown in Fig. 10(a). Particles are injected along $\pm x_d$ with $\phi = \mp 90°$, and each particle follows its neutral axis until a deflection force is introduced at $z/(\beta\lambda)$ = 2.75 to deflect them toward the z-axis. This force is generated by programming the parameter α, which changes the deflection parameter D. The variation of α is shown in Fig. 10(b). To funnel rapidly, large changes are made in α to first deflect both particles toward the z-axis, and then at $z/(\beta\lambda) = 4.75$, α is reversed in sign to provide both particles with a deflection force away from the z-axis. Finally, at $z/(\beta\lambda) = 7.75$, α is made equal to zero at the funneling vertex where both particles have reached the z-axis with zero slope. The forces required to funnel extend from $z/(\beta\lambda) = 2.75$ to 7.75, or 5.0 focus periods. The betatron period is 24 focus periods, so that the funneling operation required 21% of a period. In this example, there was no change in the longitudinal velocity because synchronous particles of $\phi = \pm 90°$ were injected so that $\bar{E}_z \equiv 0$. Figure 10(a) also shows the RFQ pole-tip shape in the x-z plane. The cross-hatched poles are plotted with the same vertical scale as

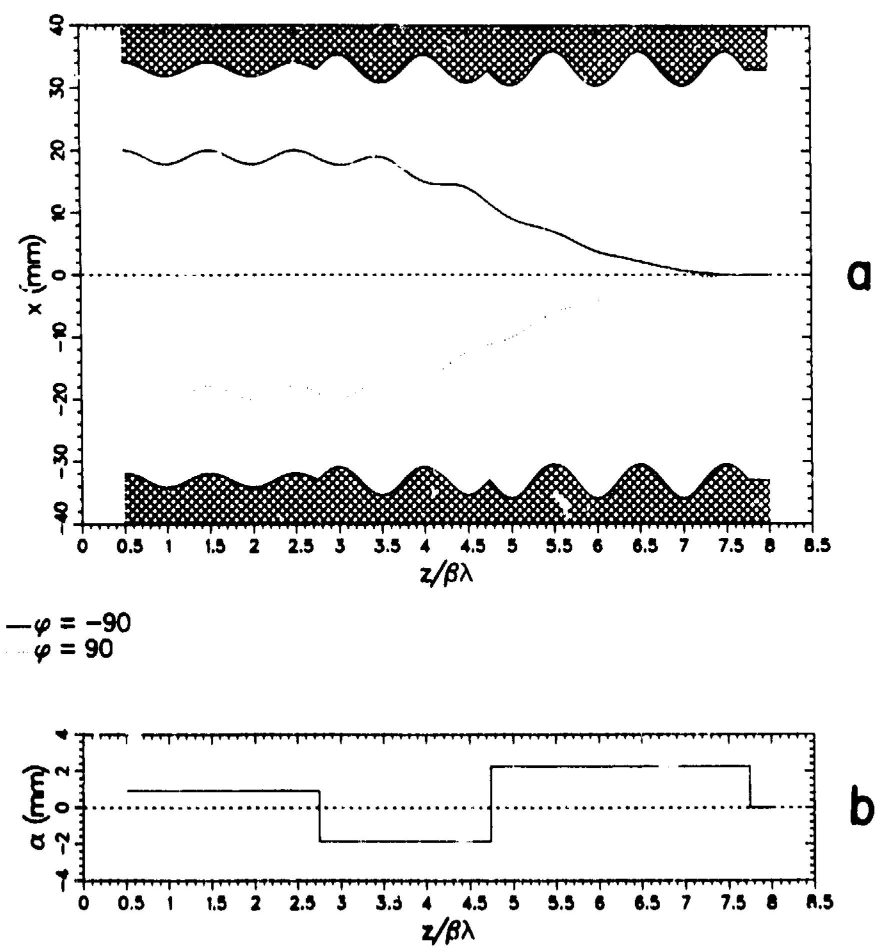

Fig. 10. RFQ funnel calculated trajectories. In Part (a), particles are injected on either side of the z-axis with $\phi = \pm 90°$. They are then deflected so that they reach the axis with zero slope to form a collinear beam of interlaced microstructure pulses. Part (b) shows the programming of the lens displacement parameter α necessary to provide the appropriate deflections. During the process, all particles will be subject to uninterrupted transverse focusing toward their respective central trajectories.

that of the particle trajectories. At two places, the poles have a sharp cusp-like shape that would not be acceptable from the standpoint of rf breakdown criteria. These cusps are an artifact of using square-wave programming for α. This situation can easily be avoided by appropriate smoothing.

Another set of calculated trajectories is shown in Fig. 11(a), with the programming of x for φ = -90° shown in Fig. 11(b). To illustrate the effectiveness of the transverse focusing throughout the funneling process, we initiated all the trajectories one-half betatron wavelength ahead of the funneling vertex. First, trajectories with zero betatron amplitude were calculated for beams on either side of the z-axis. Then for positive x, two trajectories

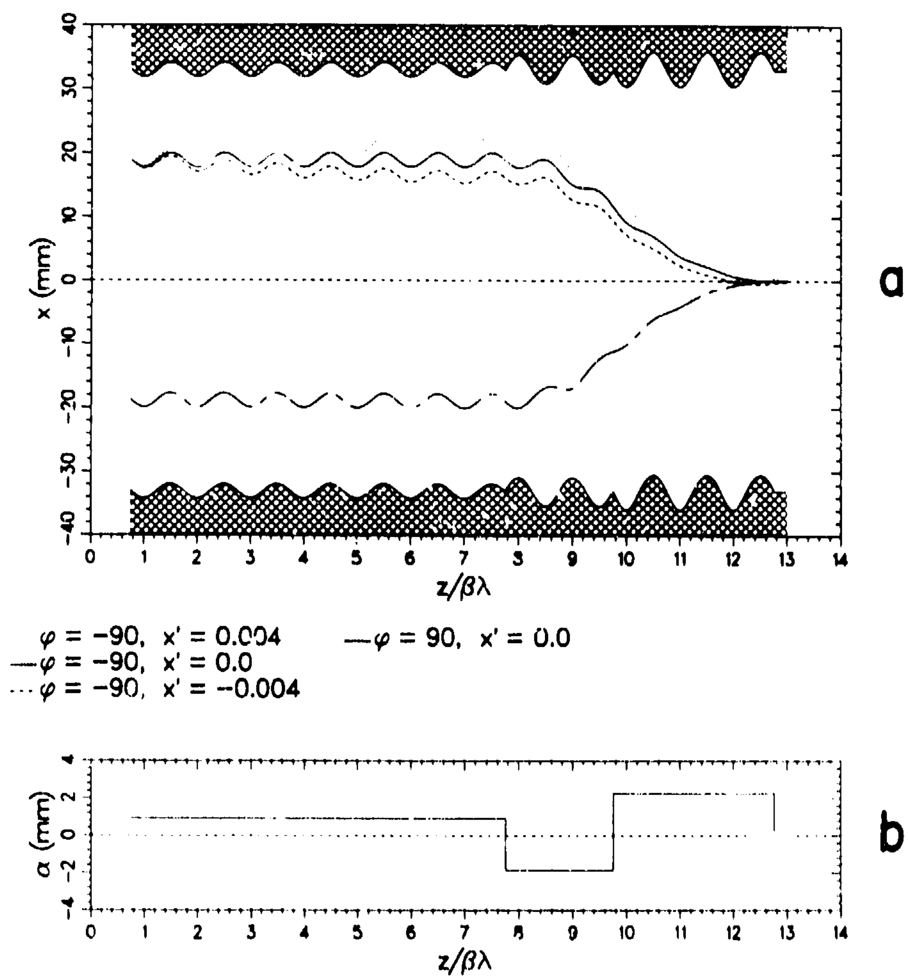

Fig. 11. Demonstration of the transverse focusing properties of the RFQ funnel. In Part (a), trajectories were calculated for particles injected one-half betatron wavelength ahead of the funneling vertex. All trajectories reach the z-axis at the funneling vertex, which shows the continuous nature of the transverse focusing with negligible effects from field nonlinearities. In Part (b) the programming of α is shown for φ = -90°.

with finite betatron amplitude were calculated to observe the effect of transverse focusing on a beam of non zero emittance. Both trajectories reach the z-axis at the funneling vertex. This result is similar to Fig. 5, except that electric field nonlinearities whose magnitude depend upon kx could perturb the betatron period and produce emittance growth. For the trajectories of Fig. 11, kx varied from 0.63 to zero; and the absence of nonlinearity effects suggests that RFQ funneling can be accomplished at appreciably large values of kx. This means that beams can be combined in a funnel of reasonably large aperture without requiring especially high ion velocities or low RFQ frequencies.

The funneled beam has unusual transverse phase-space characteristics. At the funnel output in a specific transverse plane, successive microstructure pulses have alternating phase-space ellipse parameters. In this situation one must use time-varying optical elements to match the beam. One possibility is to use a radial matching section* similar to that used at the input of an RFQ accelerator. Adding such a radial matching section to the RFQ funnel output will make all pulses have identical ellipse parameters and will produce an output beam equally divergent in both transverse planes. Then, a solenoid to produce a convergent beam will allow it to be matched to an RFQ accelerator operating with frequency 2f. The 2f RFQ accelerator would consist of an input radial matching section, a rebuncher, and a final accelerator section that could feed another funnel or an Alvarez linac.

CONCLUSION

To funnel high-current, low-emittance ion beams at low velocities, we have proposed a new type of RFQ structure and have investigated its beam-dynamical properties. This RFQ provides strong electric periodic focusing to the ion beams, and at the same time provides the transverse deflection forces necessary to merge two bunched beams into a single beam with interlaced microstructure pulses. The mechanical and rf design for the RFQ funnel should be greatly facilitated by the widespread active development of the RFQ accelerator. It should be feasible to apply existing technology in the areas of pole-tip construction, resonator design, and rf power. Also, RFQ accelerator beam-dynamics design and analysis techniques such as the RFQUIK and PARMTEQ programs can be adapted. These practical considerations, as well as the intrinsic properties of the RFQ funnel, should make it an attractive candidate for increasing beam brightness.

APPENDIX A

ALTERNATIVE FUNNELING POTENTIAL FUNCTION

A second RFQ potential function that may be useful for funneling is

$$U = \frac{V}{2} \left[G \frac{2xy}{a^2} + H \sinh kx \cos kz\right] \sin (\omega t + \phi) \quad .$$

The second term is identical to that of Eq. (5), but the quadrupole focusing term has been rotated 45° about the z-axis. In this case, periodic modulation of the poles in the y-direction produces deflection forces in the x-direction. This is a new geometry that could be advantageous in certain applications. Using the above potential function allows replacement of one pair of poles by an isopotential conductor in the y-z plane, which permits acceleration, bunching, and focusing of a single displaced beam with only two poles, plus the isopotential plane.

APPENDIX B

FUNNELING RFQ POLE-TIP SHAPES

To find the shape of the isopotential surfaces of the RFQ poles, we use Eq. (5) and set U(max) = V/2 to obtain

$$\frac{C}{a^2}(x^2 - y^2) + D \sinh kx \cos kz = 1 \quad . \tag{A-1}$$

Let $y = 0$ and set $x = a$ for $z = 0$, and $x = ma$ for $z = \beta\lambda/2$. We then obtain expressions for the coefficients C and D:

$$C = 1 - D \sinh ka \quad , \qquad D = \frac{m^2 - 1}{m^2 \sinh ka + \sinh mka} \quad .$$

Numerical solutions of Eq. (A-1) were used to calculate the electrode shapes shown in Figs. 7 and 8. Although these figures for illustration use a large value of the deflection parameter m, often much smaller values will be sufficient to produce the desired deflection force. For example, if the phase advance per focusing period is 36°, $ka = 0.1$, and $\phi = -90°$, the neutral axis is displaced by a/2 if $m = 1.14$.

REFERENCES

1. D. E. Young, Proc. Heavy Ion Fusion Workshop, Brookhaven National Laboratory report, BNL-50769, 17, (1977); R. Kustom et al., ibid., 94; D. A. Swenson, Proc. Heavy Ion Fusion Workshop, Lawrence Berkeley Laboratory report, LBL-10301 and Stanford Linear Accelerator Laboratory report, SLAC-PUB-2575, 239, (1979).

2. K. Bongardt, Proc. 1984 Linac Conf., Gesellschaft für Schwerionenforschung, Darmstadt report GSI-84-11 (September 1984), 389.

3. F. W. Guy and T. P. Wangler, and F. W. Guy, these proceedings.

4. E. A. Knapp and R. A. Jameson, Accelerator Technology Program, January-June 1981, p.46, Los Alamos National Laboratory report LA-9320-PR (May 1982).

5. I. M. Kapchinskii and V. A. Teplyakov, Prib. Tekh. Eksp. No. 2, 19-22 (1970).

6. K. R. Crandall, R. H. Stokes, and T. P. Wangler, Proc. 10th Linear Accelerator Conf., Brookhaven National Laboratory report, BNL-51134, 205 (1979).